Aircraft initial mass estimation using Bayesian inference method

Article *in* Transportation Research Part C Emerging Technologies · May 2018

DOI: 10.1016/j.trc.2018.02.022

CITATIONS
60

READS
1,647

3 authors:

Junzi Sun
Delft University of Technology
66 PUBLICATIONS **923** CITATIONS
SEE PROFILE

Joost Ellerbroek
Delft University of Technology
142 PUBLICATIONS **2,385** CITATIONS
SEE PROFILE

Jacco Hoekstra
Delft University of Technology
148 PUBLICATIONS **2,570** CITATIONS
SEE PROFILE

Aircraft Initial Mass Estimation Using Bayesian Inference Method

Junzi Sun, Joost Ellerbroek, Jacco Hoekstra
Control and Simulation, Faculty of Aerospace Engineering
Delft University of Technology, the Netherlands

Abstract

Aircraft mass is a crucial piece of information for studies on aircraft performance, trajectory prediction, and many other topics of aircraft traffic management. However, It is a common challenge for researchers, as well as air traffic control, to access this proprietary information. Previously, several studies have proposed methods to estimate aircraft weight based on specific parts of the flight. Due to inaccurate input data or biased assumptions, this often leads to less confident or inaccurate estimations. In this paper, combined with a fuel-flow model, different aircraft initial masses are computed independently using the total energy model and reference model at first. It then adopts a Bayesian approach that uses a prior probability of aircraft mass based on empirical knowledge and computed aircraft initial masses to produce the maximum a posteriori estimation. Variation in results caused by dependent factors such as prior, thrust and wind are also studied. The method is validated using 50 test flights of a Cessna Citation II aircraft, for which measurements of the true mass were available. The validation results show a mean absolute error of 4.3% of the actual aircraft mass.

keywords - aircraft mass, weight estimation, Bayesian inference

---

The article is published by Elsevier *Transportation Research Part-C*. The publisher's version can be found at Elsevier website: https://doi.org/10.1016/j.trc.2018.02.022

Nomenclature

$\boldsymbol{m}$	Aircraft mass	kg
$\boldsymbol{\eta}$	Thrust coefficient	-
$\boldsymbol{T}$	Total dynamic thrust	N
$\boldsymbol{T_\infty}$	Maximum static thrust	N
$\boldsymbol{D}$	Total drag force	N
$\boldsymbol{L}$	Aircraft lift force	N
$\boldsymbol{\mu}$	Runway friction coefficient	-
$\boldsymbol{a}$	Aircraft acceleration	m/s^2
$\boldsymbol{V}$	True airspeed	m/s
$\boldsymbol{V_z}$	Vertical speed	m/s
$\boldsymbol{C_D}$	Drag coefficient	-
$\boldsymbol{C_L}$	Lift coefficient	-
$\boldsymbol{C_{d0}}$	Zero lift drag coefficient	-
$\boldsymbol{C_{di}}$	Induced drag coefficient	-

1 Introduction

Aircraft mass is a fundamental parameter for studies on aircraft performance and trajectory prediction. However, data concerning the mass of almost all modern commercial flights are treated as confidential information by airliners, which poses a challenge for the research community. Studies from Jackson et al. (1999) and Coppenbarger (1999) have shown that having inaccurate aircraft mass estimations introduces a significant source of error, which affects ground based trajectory predictions. The study of Thipphavong et al. (2012) implemented an adaptive aircraft weight algorithm to improve the accuracy of climbing predictions. Fricke et al. (2015) illustrated the significant influence of aircraft mass on fuel burn during continuous descent operations.

Within the air traffic management research community, several methods have been developed to estimate aircraft mass based on flight data, either from radar data or more recently from ADS-B data. In two separate studies, Alligier et al. (2013, 2015) developed a least-squares method and a machine-learning method, which focused on the climb phase of aircraft. In a similar approach considering climbing aircraft, Schultz et al. (2012) implemented an adaptive estimation method for mass and thrust approximation. More recently, Sun et al. (2016) used ADS-B data from takeoff to estimate the initial mass of an aircraft with two different analytical methods. On the operational side, a different approach has been proposed by Lee & Chatterji (2010), which tries to calculate the weight of an aircraft based on an approximation of each individual weight component, i.e. aircraft empty weight, fuel weight, and payload weight.

For most of these studies, the focus was on a specific part of the flight (takeoff or climb). It is often not possible to produce a reasonable estimate for individual flights. One can only infer the possible distribution of aircraft mass based on a great number of flights. This is not only due to the variance in the data, but also due to uncertainties in aircraft configuration, something that is suggested in all of these studies. To develop a method that can estimate the mass of any flight becomes the focus of this paper.

In a preliminary study presented earlier by Sun et al. (2017*a*), the use of multiple mass estimations was identified as a potential improvement for mass estimation, studying not just one specific flight phase, but a combination of all phases. This allows more insight into aircraft mass to be inferred. In this paper, the mass estimation problem is considered as a single parameter Bayesian

inference problem (Gelman et al. 2014, p.29), considering masses computed along the entire flight as 'observations'. In addition to multiple observations, prior knowledge on weight can be used to improve the estimation. For instance, aircraft will never operate above their maximum takeoff weight or below their minimum operational weight. In practice, given an approximation of the number of passengers, one can even further constrain the weight estimation range by making an estimate of the aircraft payload. These kinds of prior knowledge can be very valuable for estimation of actual aircraft mass when applying Bayesian inference.

The remainder of this paper is structured as follows: first, this paper presents several existing methods to calculate aircraft mass independently in each flight phase. Then, in Section three, a Bayesian inference approach is established to use these calculations as independent measurements, combining a priori knowledge of initial aircraft mass probability distribution to produce a maximum a posteriori estimation. The advantage of the Bayesian approach is that it takes into account prior probability distribution and physical limitations of possible aircraft mass. It has the potential to produce an estimate for any given flight based on flight data with the knowledge of aircraft type. Figure 1 gives an illustration of this method.

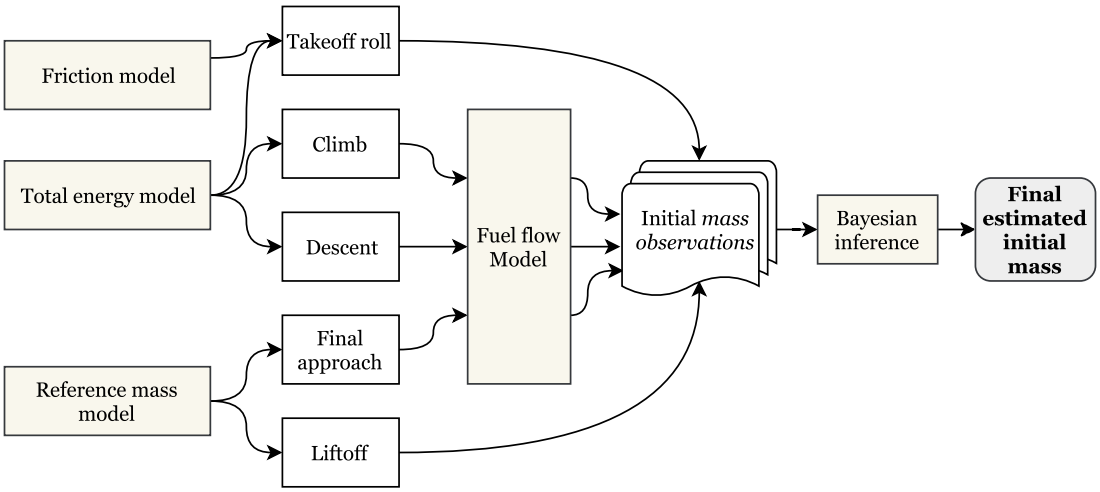

Figure 1: Flow chart of the estimation structure

Section four discusses the results for several aircraft types and parameter sensitivities. Section five uses a real flight dataset to validate the Bayesian inference method. Finally, discussion and conclusions are presented in sections six and seven.

2 Individual aircraft mass estimates

This section describes five methods that can be used independently to compute aircraft mass at different flight phases. The total energy model (TEM), shown in Equation 1, is used in most of the methods. In addition, BADA3 aerodynamic coefficients are used to calculate the thrust and drag in some of the phases when applicable (Nuic 2014).

$$
\begin{aligned}
(T-D)\cdot V &= m\cdot a\cdot V + m\cdot g\cdot V_z \\
D &= C_D\cdot\frac{1}{2}\rho V^2 S \\
L &= C_L\cdot\frac{1}{2}\rho V^2 S \\
C_D &= C_{d0}+C_{di}C_L^2
\end{aligned}
\tag{1}
$$

Here, T and D are the thrust and drag of the aircraft, V, a, and V_z are the airspeed, acceleration, and vertical rate respectively. C_D, C_L, C_{d0}, and C_{di} are coefficients for drag, lift, zero lift drag, and lift-induced drag. ρ and S are the air density and the aircraft reference wing surface. In addition, the forces acting on an airborne aircraft are also illustrated in Figure 2.

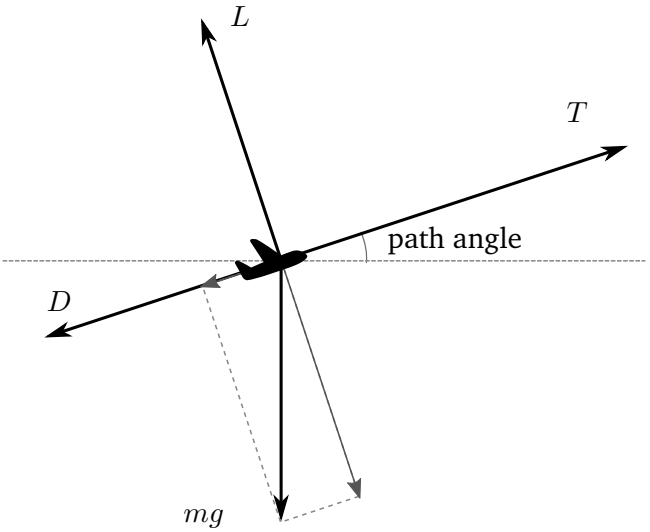

Figure 2: Forces acting on an airborne aircraft (climb)

With the complete flight trajectory based on the total energy model, mass can be computed at different phases as illustrated in Figure 3, where the subscripts *TO, LOF, CL, DE,* and *APP* represent takeoff, liftoff moment, climb, descent, and final approach, respectively. A fuel flow model is used together with these estimates to generate independent 'observations' of the initial mass at takeoff for further Bayesian inference.

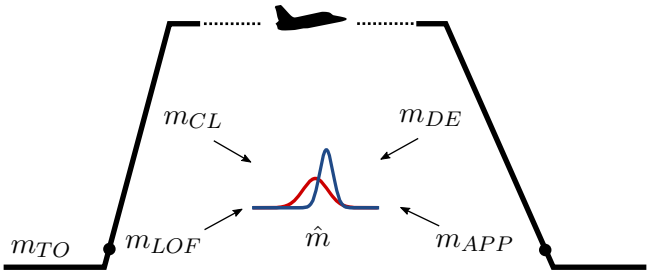

Figure 3: Bayesian inference using multiple mass observations

In the rest of this paper, the term *mass observation* is used for initial masses that are computed at different stages of the flight in combination with the fuel flow, as illustrated in Figure 1. It is worth noting that these *mass observations* are not directly observed, but calculated using the deterministic

total energy equations. These values are independently calculated, which means that there is no data overlap between the computed *mass observations*. The remainder of this section discusses how initial masses are computed deterministically.

2.1 Taking off

While an aircraft is on the runway before liftoff, it only accelerates horizontally. Because it is still on the ground, ground friction needs to be considered in addition to the aerodynamic drag. This ground friction is proportional to the normal force on the ground, with a friction coefficient denoted by μ_1. A common value is around 0.02 for concrete runways (Wetmore 1937). Equation 1 then can be re-written as follows:

$$T - D - D_g = ma \tag{2}$$

$$D_g = \mu_1(W - L) \tag{3}$$

Due to the fact that BADA (version 3) does not have an accurate thrust model for the ground phase at takeoff, thrust needs to be computed with other models. Alternatively, the maximum take-off thrust can be calculated from empirical data using a second-degree polynomial model (Bartel & Young 2008). This approach provides a fairly good approximation of thrust for two-shaft turbo-fan engines. This simplified model can later be used during other phases of flight. The maximum takeoff thrust can be expressed as a function of velocity:

$$T_{max} = f(V) = T_\infty(1 + c_1 V + c_2 V^2) \tag{4}$$

where T_∞ is the maximum static thrust at sea level. Parameter c_1 (negative value) and c_2 (positive value) are coefficients obtained from empirical data fitting that are dependent on the engine bypass ratio (Bartel & Young 2008). During takeoff, the optimal lift coefficient can be derived. Equation 2 is rewritten as follows:

$$\begin{aligned} T &= D + D_g + ma \\ &= \frac{1}{2}\rho V^2 S(C_{d0} + C_{di}C_L^2) + \mu_1(mg - \frac{1}{2}\rho V^2 S C_L) + ma \\ &= \frac{1}{2}\rho V^2 S(C_{d0} + C_{di}C_L^2 - \mu_1 C_L) + \mu_1 mg + ma \end{aligned} \tag{5}$$

For a given velocity V, T is minimum when C_L satisfies the following equation (Mair & Edwards 1965):

$$C_L = \frac{\mu_1}{2K} \qquad (\frac{dT}{dC_L} = 0) \tag{6}$$

When the requirement of minimum excess thrust is satisfied, aircraft can take off with reduced thrust. This has become common practice for airliners to extend engine life and reduce costs. To accommodate this possibility in the model, a thrust coefficient η is introduced that satisfies $\eta \leq 1$. Combined with Equation 6, Equation 5 becomes:

$$\eta T_{max} - (\mu_1 g + a)m - \tfrac{1}{2}\rho V^2 S(C_{D0,to} - \frac{\mu_1^2}{4K_{to}}) = 0 \tag{7}$$

Let the left part of the equation be $\boldsymbol{f}_1(m, \eta)$. The task is to find the optimal $\hat{m}$ and $\hat{\eta}$ that minimize the squared sum of $\boldsymbol{f}_1$ of all takeoff data samples. The solution can be found as follows, with constraints on m and η.

$$\begin{aligned} \hat{m}, \hat{\eta} &= \arg\min_{m,\eta} \sum_{i=1}^{N} \boldsymbol{f}_1^2(m, \eta) \\ m &\in (0, c_m) \\ \eta &\in (c_\eta, 1) \end{aligned} \tag{8}$$

where the η constraint represents the possible reduction of thrust during the takeoff and the range of m represents a very large mass range. The coefficients c_m and c_η are user-defined boundary conditions. The quality of the optimization solution depends on the accuracy of the velocity measurements and the number of data samples. It is possible that an optimal mass solution may not be found and that the optimization, instead, converges to the condition boundaries. In this paper, a *mass observation* at the boundary conditions (zero or $2m_{mtw}$) is considered as an *impossible observation*.

2.2 Liftoff and final approach

At each liftoff and final approach, optimal speeds are usually selected, which are correlated to the stall speed. Even though it is a relatively weaker correlation at takeoff, both speeds can be used as indicators to infer aircraft mass.

This method first observes the aircraft liftoff speed (airspeed at which the aircraft first becomes airborne) and speed of final approach. Then it infers the mass taking into account the relationship with stall speed at maximum takeoff or the landing weight when it is available from the aircraft manufacturer. When these parameters are not available, BADA reference data are used.

According to the FAA Federal Aviation Regulations, at takeoff, the speed of an aircraft is at least 20% over the stall speed. Assuming lift and weight are the same at liftoff, the following relation can be derived under certain assumptions:

$$\begin{aligned} W_{to} = L_{to} \quad &\Rightarrow \quad m_{to} g = \frac{1}{2} \rho S C_L V_{lof}^2 \\ &\Rightarrow \quad m_{to} \propto V_{lof}^2 \end{aligned} \tag{9}$$

where the takeoff mass is proportional to the liftoff speed squared, under the assumptions of the same aircraft model and lift configurations. Knowing reference weight and corresponding stall speed (V_S), it is possible to calculate such a constant coefficient:

$$C = \frac{m_{to}}{V_{lof}^2} \tag{10}$$

$$= \frac{m_{ref,lof}}{V_{ref,lof}^2} \leq \frac{m_{ref,lof}}{1.2^2 \cdot V_{S,ref,lof}^2} \tag{11}$$

Then at any given observed takeoff, the initial mass can be approximated using the following equation:

$$m_{to} \approx \left(\frac{m_{ref,lof}}{1.2^2 \cdot V_{S,ref,lof}^2} \right) V_{lof}^2 \tag{12}$$

A similar relationship can be obtained at landing. The approach speed empirically is around 30% over the stall speed. The landing mass then can be approximated as follows:

$$m_{ld} \approx \left(\frac{m_{ref,app}}{1.3^2 \cdot V_{S,ref,app}^2} \right) V_{app}^2 \tag{13}$$

Such approaches are also briefly addressed in previously mentioned research by Fricke et al. (2015). When using ADS-B data, it is common that there is a certain gap between the on-ground data and in-air data. Hence, the liftoff speed and approach speed can be obtained using a interpolation method based on several data points during takeoff or landing. This method is described by Sun et al. (2017*b*).

2.3 Climb and descent phase

During the climb and descent phases, horizontal speed and climb/descent rate observations can be employed to estimate aircraft mass. Assuming standard atmospheric conditions, the total energy model in Equation 1 can be expanded at each time step as follows:

$$\begin{aligned}
(T_i - D_i)\, V_i &= m_i a_i V_i + m_i g V_{zi} && (14)\\
m_i &= m_0 + m_{i,fuel} && (15)\\
T_i &= \eta T_{max,i} \;=\; \eta f(h_i, V_i) && (16)\\
D_i &= C_D \; \frac{1}{2} \rho_i V_i^2 S && (17)\\
L_i &= m_i g \cos(\gamma_i) \;=\; C_{L,i} \; \frac{1}{2} \rho_i V_i^2 S && (18)\\
C_D &= C_{d0} + C_{di} C_{L,i}^2 && (19)
\end{aligned}$$

Here, γ represents the flight-path angle. Maximum thrust profile T_{max} is a function of pressure altitude and airspeed and η is an assumed thrust coefficient for the entire climb or descent, describing the actual thrust setting as a percentage of maximum thrust. Given all observed and known variables, the above equations can be rewritten into the following equation:

$$\begin{aligned}
&\frac{2kg^2 \cos^2(\gamma_i)}{\rho_i V_i^2 S} \cdot m_i^2 + \left(a_i + g \frac{V_{zi}}{V_i} \right) \cdot m_i \\
&\qquad + C_{d0} \; \frac{1}{2} \rho_i V_i^2 S - \eta \cdot T_{max,i} = 0
\end{aligned} \tag{20}$$

Fuel consumption can be estimated according to Section 2.4, where the last remaining two unknown variables m_0 and η are to be found. This process is similar to the takeoff method but includes more parameters in the equation. Let the left side of Equation 20 be $\boldsymbol{f}_2(m, \eta)$. The task is to find the optimal $\hat{m}$ and $\hat{\eta}$ that minimize the squared sum of $\boldsymbol{f}_2$ of all N data samples. The mass is constrained by the aircraft Operational Empty Weight and the Maximum Takeoff Weight, and thrust reduction is no larger than 20% of the maximum thrust profile. The solution can be found as follows for climbing flights:

$$\begin{aligned}
\hat{m}_0, \hat{\eta} &= \underset{m_0, \eta}{\arg\min} \sum_{i=1}^{N} \boldsymbol{f}_2^2(m_0, \eta) && (21)\\
m &\in (0, c_m)\\
\eta &\in (c_\eta, 1)
\end{aligned}$$

Although the total energy equation is the same for descent flights, their thrust profiles are different. In the above equations, $\eta \cdot T_{max,i}$ needs to be replaced with idle thrust or appropriated thrust setting in the case of powered descent. In this paper, unless specified, idle thrust is assumed during descent.

Compared to the takeoff phase, climb and descent usually last for a significantly longer time, where a large number of data samples can be gathered. Rather than using all data from the entire climb or descent for the calculation, these data can be split into smaller segments which produce multiple *mass observations*. One way to split the data is according to the continuous climb/descent segments and level flight segments. Another way to split the data is to produce equal-length data chunks. Finally, a combination of both approaches may also apply. This practice is useful to generate larger numbers of *mass observations*. In this research, the first approach to split the data based continuous climb or descent segments is recommended. This way, less operation maneuvers are expected in each segments.

2.4 Fuel burn model

When considering an entire flight from takeoff to landing, aircraft mass varies as a function of fuel burn. For an aircraft that is taking off or during initial climb, one can assume the mass is the same as initial mass. However, for mass that is derived from the rest of the climb phase, the descent phase, and the final approach, the consumption of fuel need to be taken into account when inferring the initial mass of the aircraft. This is illustrated in the general estimation flowchart (in Figure 1). With a fuel burn model, the initial mass of an aircraft can be computed as the sum of flow consumption and the mass computed at a given point of the flight.

Several studies have been conducted to estimate fuel burn. Methods have been proposed that are based on radar track data (Chatterji 2011), as well as a classification model from the Flight Data Recorder (Chati & Balakrishnan 2016). Other fuel flow calculation models obtained from empirical data can be found in BADA and the ICAO aircraft engine emission data-bank (ICAO 2016). In the following sections, both ICAO and BADA models are introduced, while the ICAO model will be used in practice considering its open accessibility.

2.4.1 BADA3 fuel flow model

The BADA3 calculation consists of three fuel flow modes, minimal (idle thrust at descent), cruise (cruise thrust), and nominal (other flight phases). With the BADA model, fuel flow can be calculated based on the flight data. It produces a relatively higher-accuracy result with better trained models. Details of BADA fuel flow calculations can be found in the BADA user manual. In summary, BADA computes the fuel flow as a function of aircraft speed and thrust during the taking off and climbing or a function of altitude form cruising and idle descent. Different coefficient values are given for each aircraft type.

2.4.2 ICAO fuel flow model

The ICAO engine emission data-bank defines fuel flow under four different modes: takeoff, climb-out, approach, and idle, with power settings at 100%, 85%, 30%, and 7% of engine maximum power respectively. It is important to note that all data are gathered from static engine tests. Hence, the fuel flow measurements are biased compared to dynamic flight data.

In order to get the model closer to actual fuel consumption, based on the four points from the ICAO data bank, a quadratic fuel flow profile is constructed describing the fuel flow as a function of the fraction between actual thrust T and maximum static thrust T_∞, denoted as ϵ:

$$\dot{m}_{fuel} = K_1\epsilon^2 + K_2\epsilon + K_3 \tag{22}$$

From the ICAO data bank, fuel flow data are fitted with a polynomial model for several engines. Figure 4 shows the results of the fitted model obtained from data from several engines and their corresponding aircraft types.

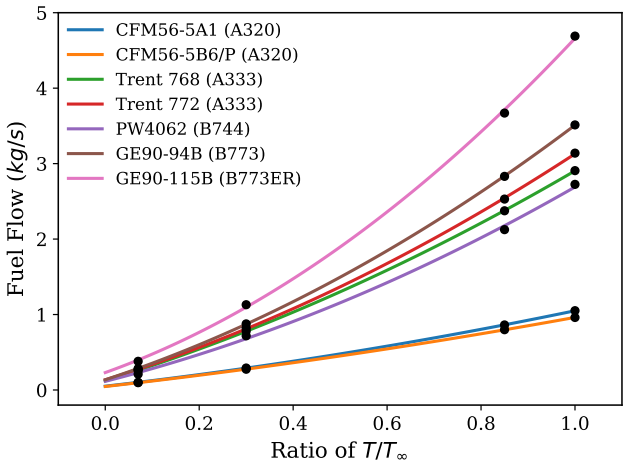

Figure 4: ICAO fuel flow interpolation

For a common two-shaft turbofan engine it is possible to simplify the thrust model using an empirical relation (Bartel & Young 2008) between aircraft Mach number and pressure altitude (en-route flights), which can be calculated from the ADS-B data assuming standard atmospheric conditions.

$$\epsilon = \frac{T}{T_\infty} = f_1(M, H) \tag{23}$$

Thus the actual fuel burn can be calculated as a function f_2 of Mach number, altitude, and time obtained from the flight data. Finally, the consumed fuel mass can be integrated throughout the flight at any given time τ:

$$m_{fuel} = \int_0^\tau f_2(M, H)dt \tag{24}$$

Because it is a model built on open data, the ICAO model is used in this paper. It is worth to mention that this model contains a certain level of inaccuracy based on previous studies. Research on operational flight data and tests conducted by Zürich Airport (Fleuti & Polymeris 2004) have shown that there is a difference between the ICAO fuel flow model and operational fuel consumption. An average of 38% of difference (less in operation in comparation to ICAO) in fuel consumption LTO (Landing and Takeoff) cycle is found by this report. However, the difference of en-route flight fuel consumption is not studied, thus remains unknown from this literature.

With the polynomial fuel flow model based on ICAO data-bank proposed earlier, this paper no longer relies on the discrete four-point measurements. The fuel consumption is now approximated more accurately as a continuous function in relation to the dynamic thrust of the engine.

Once the total fuel burn can be computed at any give time according to 24, denote a computed mass m_τ (in climb, descent, or approach) at time τ, the initial mass (m_*) becomes:

$$m_* = m_\tau + m_{fuel} = m_\tau + \int_0^\tau f_2(M, H)dt \tag{25}$$

3 Bayesian Inference

As shown in the last component of the estimation flowchart (Figure 1), the final estimate is computed using Bayesian inference. The Bayesian inference uses Bayes' theorem (Bayes et al. 1763) to update a hypothesis probability based on evidence (or observation). In the case of estimating aircraft mass, it uses computed mass at each flight phase to update an initial belief. This belief is called *prior* in Bayesian terms. The prior essentially describes the probability density function of a parameter before any observation is made.

To understand the process, first, let us assume n possible *mass observations* are obtained from different flight phases:

$$\boldsymbol{m} = m_1, m_2, \cdots, m_n \tag{26}$$

These observations are possible values of initial aircraft mass. However, due to errors in aircraft flight data and estimations, those values can be very different from reality or even out of the physical boundaries. If, for simplicity, one assumes the observed aircraft mass follows a normal distribution:

$$m \sim \mathcal{N}(\mu, \sigma^2) \tag{27}$$

where the μ parameter refers to the underlying real aircraft mass and σ^2 is the variance of the observations.

The simplest unbiased estimate for μ is to compute the mean of $\boldsymbol{m}$, which is topically known as *Maximum Likelihood Estimate* (MLE). However this means the observations are used under the assumption that all values of μ are equally likely. In this case, the a priori knowledge of aircraft is discarded.

The Bayesian inference method introduces a prior probability function for the parameters μ and σ^2. The posterior probability function $p(\mu, \sigma^2|\boldsymbol{m})$ is computed as the probability of μ based on observed measurements. The most likely value in the posterior distribution function (the mode) is denoted as the *Maximum a Posteriori Probability Estimate* (MAP). The MAP can also be seen as a regularization of the MLE, due to the additional information of prior knowledge introduced.

3.1 Normal prior with fixed variance

First, to deduce the simplest closed form of the posterior function, the fixed variance (a chosen σ^2) assumption is used. Let the prior probability function for μ be defined as follows:

$$\mu \sim \mathcal{N}(\mu_0, \sigma_0^2) \tag{28}$$

Following the derivation in Sun et al. (2017*a*), the posterior probability distribution of μ satisfies

the following normal distribution:

$$\begin{aligned} \mu|\boldsymbol{m} &\sim \mathcal{N}\left(\frac{n\sigma_0^2\bar{m}+\sigma^2\mu_0}{\sigma^2+n\sigma_0^2}, \quad \left(\frac{1}{\sigma_0^2}+\frac{n}{\sigma^2}\right)^{-1}\right) \\ \bar{m} &= \frac{1}{n}\sum_1^n m_i \end{aligned} \tag{29}$$

where n is the number of the measurements and $\bar{m}$ is the mean of all measurements. An example will be given in the next section.

3.2 Normal distribution with unknown variance

When the variance is also to be assumed unknown, in order to obtain the closed-form solution, the conjugate prior distribution is a four-parameter Normal-Gamma distribution. The likelihood of any mass m_i is:

$$m_i|\mu,\tau \sim \mathcal{N}(\mu, 1/\tau) \tag{30}$$

where τ is the equal to $1/\sigma^2$. The Normal-Gamma (NG) prior distribution for μ and τ is defined as follows:

$$\mu,\tau|\mu_0,\lambda_0,\alpha_0,\beta_0 \sim \mathcal{N}(\mu|\mu_0, 1/(\lambda_0\tau))\; G(\tau|\alpha_0,\beta_0) \tag{31}$$

where $G(\cdot|\alpha,\beta)$ is the Gamma distribution described by shape α and rate β. From all the observations $\boldsymbol{m}$, the posterior distribution can be calculated as follows, where the detailed derivation can be found in Murphy (2007):

$$\begin{aligned} \mu,\tau|\boldsymbol{m} &\sim NG(\mu,\tau|\mu_1,\lambda_1,\alpha_1,\beta_1) \\ \mu_1 &= \frac{\lambda_0\mu_0+n\bar{m}}{\lambda_0+n} \\ \lambda_1 &= \lambda_0+n \\ \alpha_1 &= \alpha_0+n/2 \\ \beta_1 &= \beta_0+\frac{1}{2}\sum(m_i-\bar{m})^2+\frac{\lambda_0 n(\bar{m}-\mu_0)}{2(\lambda_0+n)} \end{aligned} \tag{32}$$

The mean μ and τ of Normal-Gamma PDF are given by:

$$\hat{\mu},\ \hat{\tau}=\mu_1,\ \frac{\alpha_1}{\beta_1} \tag{33}$$

3.3 Other types of distributions

In general cases, both the likelihood and priors are not necessarily normally distributed. Very often, a closed-form posterior distribution can therefore not be derived. This happens often when complicated models, unusual distributions, or high feature dimensions are involved. There are still ways of computing the posterior numerically. As described by Gelman et al. (Gelman et al. 2014, chap.10), several approximation algorithms have been proposed, for example, numerical integration, distribution approximation, and Bayesian sampling.

For this paper, the goal is to propose and initialize the use of prior knowledge in the computation of aircraft mass. Despite that many of these Bayesian computing techniques are available, the currently proposed method uses the simplest form of prior described earlier (Normal distributions with fixed variance). With the simple closed-form solution, the posterior can be computed fast.

4 Experiments and results

To examine and validate the Bayesian estimation approach, in total, several thousands of flights were gathered for two common aircraft types (A320 and B738). These flights were carried out between the 10th and the 16th of October, 2016. Out of all the data, the first 1500 complete trajectories for the experiment were selected. As an illustration, the great circle paths between the origins and destinations of all flights are drawn in Figure 5.

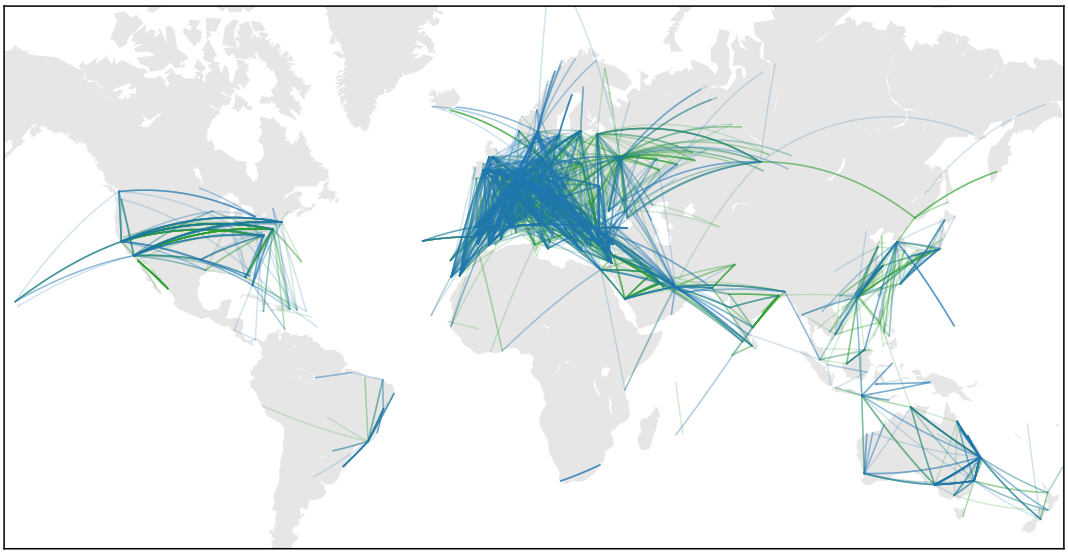

Figure 5: All flights in the data set (A320 in green, B738 in blue)

For each flight, multiple initial *mass observations* were computed at different flight phases using its respective method. After that, the Bayesian mass inference was applied. In the following part, three experiments were carried out: mass estimation for a single flight, distributions for mass estimated for all flights, and sensitivity studies. For the Bayesian inference, by default, the following values are used:

$$\begin{aligned} \mu_0 &= 65000 \text{ kg} \\ \sigma_0 &= 10000 \text{ kg} \\ \sigma &= 10000 \text{ kg} \end{aligned} \tag{34}$$

4.1 Single flight demonstrations

The Bayesian inference of two flights is illustrated in Figure 6. In the first plot, *mass observations* are computed at different flight phases. These numbers correspond to the green dashed PDF in the second plot. The prior distribution is illustrated as the dotted blue PDF on the right-hand side of the plot. The posterior is computed and illustrated by the solid red PDF.

4.2 Distributions for A320 and B737-800

Figure 7 shows the results of the inference method applied to all A320 and B738 flights in the dataset. The first five sub-plots illustrate the distribution of individual measurement results from

methods that are applied at different flight phases, which are takeoff, liftoff, climb, descent, and final approach. The last plot shows the final estimated initial masses using Bayesian inference.

By studying the results for these two different aircraft types, it is possible to conclude that at different flight phases, the initial mass computed using deterministic methods contains large variances. Some of the results are outside of the boundaries of m_{oew} and m_{mtw}. The main causes are data inaccuracy, uncertainty in the thrust, and uncertainty in the airspeed. For liftoff and final approach estimates, the margin of stall speed between the model and the actual setting may cause large inaccuracies (in the case of B737-800). A more detailed discussion for these biases is addressed in the section 6.3.

When looking at five distributions of the measurements and the final MAP estimates, it is evident that the MAP estimates have a smaller variance than the individual estimates, and most of the initial estimates are within the boundaries of m_{oew} and m_{mtw}.

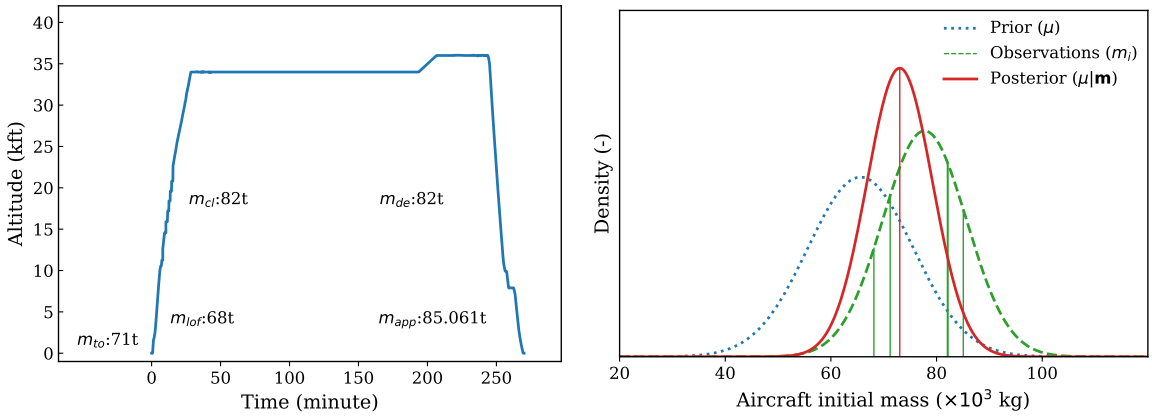

Figure 6: Example of Bayesian inference, mass observations at different phase in the first plot corresponding to the green vertical lines in the second plot

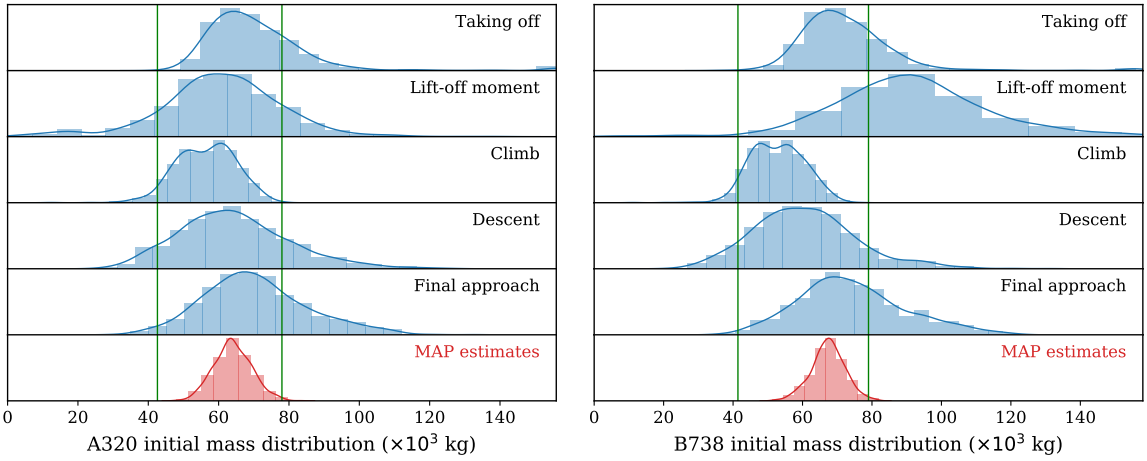

Figure 7: Comparison of estimations at different flight phases, solid vertical lines refers to the operational empty mass and maximum takeoff mass

4.3 Variation factors

In this section, the goal is to study how variations of different factors lead to changes in the estimation results, as well as the degree of these differences. Follow-on experiments are performed on the A320 dataset that was used previously.

4.3.1 Prior

When applying Bayesian inference, an important factor is the prior. A stronger belief in the prior knowledge will increase the confidence of the final estimation. However, these estimates can be biased towards the prior belief. To study this influence, the same A320 dataset is treated with a set of different priors to produce different distributions of estimates. In Figure 8, six combinations of (μ_0, σ_0) are chosen to study this effect. The probability distribution functions that are biased towards low, medium, and high mass are shown in red, black, and blue, respectively. Priors with high and low confidence are shown in solid and dashed lines, respectively.

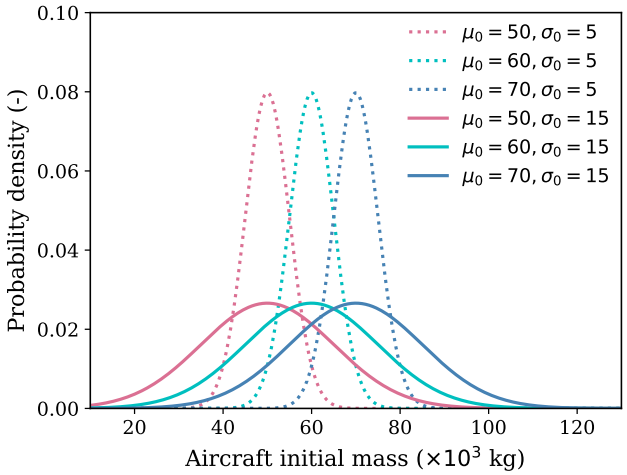

Figure 8: Different initial mass prior distribution (A320)

In Figure 9, six different results from the same estimation configuration are displayed. On the left side are plots where low confident priors (large σ_0) with different μ_0 are applied, On the right side, the results from high confident priors (low σ_0) are shown.

Results are grouped by μ_0, corresponding to the bias of the prior. On the left-hand side of the groups are distributions from lower confidence priors (higher σ_0, shown in blue), On the right-hand side of the groups are distributions with a higher confidence prior (lower σ_0, shown in orange).

From these plots, it is possible to see that with a weak prior, the estimates are less biased. They depend more on the observations (i.e.: different initial mass calculated at different flight phases). They also, in turn, produce less confident results. For instance, all three experiments end up with distributions with larger spreads. A good choice of a prior often requires some empirical knowledge with regard to the flights.

4.3.2 Thrust

The level of correctness of aircraft mass estimations based on observed performance parameters is essentially dependent on knowledge of thrust settings. As shown in Section 2, most of the

mass computation methods along the flight path need to take into account the thrust profile while estimating aircraft mass. In these methods, an optimization using the least squares method is implemented to find the best thrust setting and aircraft mass, which provides a minimal squared error. This approach has also been proposed previously Alligier et al. (2013). This approach makes sense mathematically. However, without validation using measured thrust data, it is not possible to conclude whether the thrust configuration obtained for the optimization is indeed the correct setting.

In order to study the influence of different thrust settings, based on the same dataset, two set of fixed minimum and maximum thrust profiles are used to produce two different sets of mass estimates. For takeoff and climb, maximum thrust and a 30% reduced thrust profile are used. While for descent, two thrust settings at 8% and 20% of maximum climbing thrust setting are used. In Figure 10, results from such different settings are shown, where the distributions from all flights at different flight phases are compared.

It is apparent that during the takeoff (TO) and climb (CL), higher thrust settings lead to higher estimations of initial masses, and this difference is quite significant. During the descent (DE) phase,

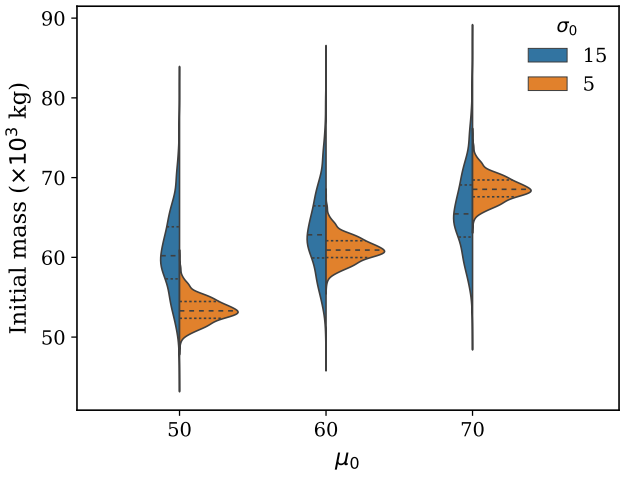

Figure 9: Variation in distributions of estimates due to different priors (A320)

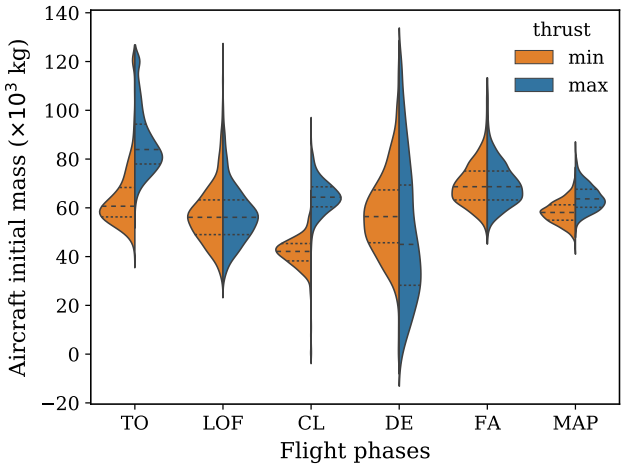

Figure 10: Sensitivity on thrust settings

Table 1: Median of estimated mass ($\times 10^3$ kg) under two thrust settings

Phase	T_{min}	T_{max}	Δm
TO	60.7	83.9	23.2
LOF	56.1	56.1	–
CL	42.1	64.4	22.3
DE	56.4	45.0	-11.4
FA	68.7	68.7	–
MAP	58.1	63.7	14.6

such a tendency is not visible. However, the uncertainty of mass estimated under high powered descent is much larger. Due the fact that thrust is not involved for estimates from liftoff (LOF) and final approach (FA), these results remain the same. When comparing these two sets of distributions, the final MAP distributions display considerable differences.

It is worth to emphasize that the mass observations obtained in this experiments are not the optimal solution in comparison with the results from Figure 7. All values are computed under a fixed thrust setting here. For the latter case, mass from the best mass/thrust pair were selected. From this test, it is possible to conclude that thrust setting is a major factor that affects the mass estimation. The link between mass and thrust should therefore not be neglected. Numerical differences (median of the distributions) are shown in Table 1.

A comparison of the distributions under two thrust settings shows that the difference in MAP is smaller than the ones seen in the previous mass observation methods. This is because under the prior assumption, measurements that are far away from a believable value are considered with lower probability. The large fluctuation caused by distinct thrust settings is reduced. Thus, more convincing distributions are produced. It is positive to see that the bias still persist in the MAP results, confirming the final result maintained the knowledge about thrust settings.

As it is common practice nowadays to apply de-rated thrust takeoff/climb to reduce engine wear, as well as minimum thrust descent to save fuel, the min thrust profile used in this experiment is closer to reality. This can be reflected in the resulting distributions, where maximum thrust profile produced much less realistic results.

4.3.3 Airspeed

All estimation methods introduced in Section 2 require correct measurements of aircraft airspeed. However, data collected from ground measurements (ADS-B or radar) only reveal the ground speed. Estimations can either assume the ground speed as airspeed or integrate wind data to approximate the airspeed. Intuitively, this uncertainty in wind can affect the estimation results.

In the experiment dataset, meteorological data are integrated with ground speed to approximate the true airspeed of aircraft. The Global Forecast System (GFS) re-analysis dataset is used to construct the wind field globally. Airspeeds of all trajectories are computed as the difference between the ground speed and wind speed.

For each flight, two sets of initial masses are computed under ground speed condition and airspeed condition. Finally, the difference in estimated mass is found and illustrated in Figure 11. It can be seen that the estimation can vary up to five metric tons of difference for the Airbus A320, which is around 6% of the maximum takeoff mass.

5 Validation with Cessna Citation flight data

As previously pointed out in the introduction section, information regarding aircraft mass from airliners are rarely available to ATM research. As a result, validations in mass estimation studies are often limited. Even when mass information would be provided by an airline, its usefulness would be limited, as this information is often computed by the Flight Management System, rather than measured. For practical reasons, airliners do not weigh cargo and passengers before taking off. Because of this, the ”true mass” data may have some level of uncertainty. A better alternative would be to perform specific flight tests, where there is more control over aircraft mass, and where true mass can be measured.

5.1 Validation dataset

The current paper used data from a set of student demonstration flights with a Cessna Citation II laboratory aircraft, to validate the proposed method. A total of 50 flights were carried out in a period of three weeks in March 2017. For each flight, the initial mass is computed as the sum of measured passenger weight, fuel weight, and aircraft basic empty weight. During the flight, a large number of flight parameters (such as fuel flow) are recorded. The average duration of the flights is approximately 80 minutes.

The demonstration flights were flown four times a day, where the aircraft was refueled between every two flights. Figure 12 shows how the initial mass varied from flight to flight. As the number of passengers was almost always the same, most of this initial mass variation is caused by the refueling schedule. Figure 12 also shows that all flights were taking off at a weight close to the maximum takeoff weight (indicated by the top solid line). It should be noted that for some of the flights (number 2, 6, 14, 27, 37, and 49), the initial fuel mass was not recorded in the flight data sheet. The amount of fuel on these flights was therefore interpolated for these flights. These data point are marked distinctly in the figure.

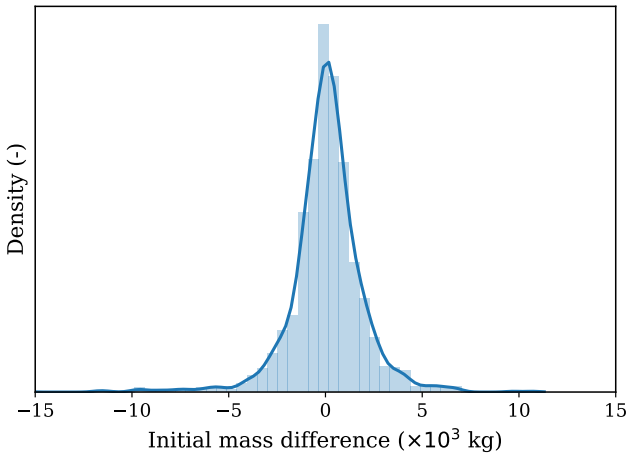

Figure 11: Difference in estimation caused by wind

5.2 Results and analysis

Figure 13 illustrates the result of Bayesian estimation applied on all flights. The difference between true mass and estimated mass is shown for each individual flight. The mean absolute error (MAE) is 4.3% of the total true mass, while all estimates are within 12% of MAE, with prior parameters of μ_0=6000 kg and σ_0=500 kg.

To assess the effect of the choice of prior, six different priors are tested with the same data, see Figure 14. Here, the plots on the right-hand side represent the distribution from different priors. Within the distribution, the scattered points are all estimated mass values. It can be seen that as expected, with the true mass as comparison, the prior that yields the best result is the one biased towards the true mass and with a high level of belief. The prior yielding the worst result is the one with a high level of belief but biased towards the wrong values. On the other hand, selecting a weak prior (larger σ_0, lower level of belief), reduces the influence of bias but increases the estimation uncertainty.

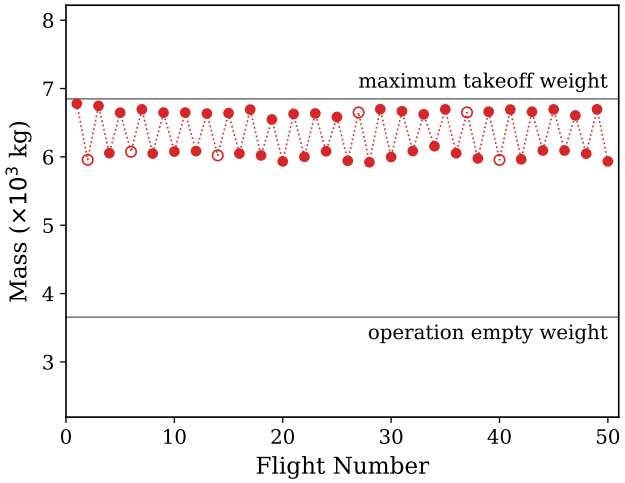

Figure 12: Aircraft initial mass for all flight

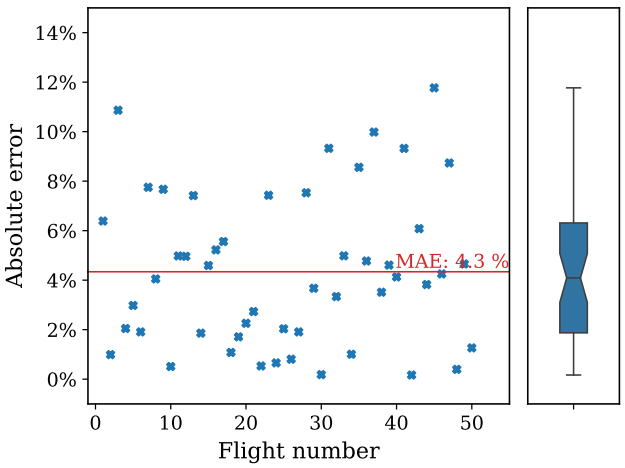

Figure 13: Bayesian estimation for all flights (prior parameters: μ_0=6000 kg, σ_0=500 kg)

6 Discussion

This paper presents a set of principles, methods, and validations for Bayesian inference of aircraft mass. From the Bayesian inference point of view, the choice of prior distribution is very important. On the other hand, related factors such as wind and thrust can influence the accuracy of *mass observations*, which can propagate to the final estimations. These factors and their limitations are addressed in this section.

6.1 Priors in Bayesian inference

The Bayesian inference approach is based on the conditional probability theory where a certain prior (or "belief") of the parameter is known. This leads the estimate to be biased to what the"belief" is. There are two ways to improve the final estimate: more measurements or a better prior when measurements are few.

Because the number of *mass observations* is low, constructing a better prior is important. In practice, other than the minimum and maximum allowed weight, one can construct the prior based on direct or indirect indicators such as historical data, occupancy, and fuel reserves. For example, for short-haul flights from low-cost airlines, a highly-biased prior towards the maximum takeoff mass can be used. One can also look at traveler statistics to construct the priors according to seasons. In the cases where the types of flight are uncertain, based on our experiments, the recommendation is to select a μ_0 around 80% of the maximum takeoff mass, and a σ_0 that is around 25% of the mass difference between the maximum and empty mass.

Normally distributed priors are assumed in this paper. The Normal distribution assumption is based on results of previous studies (Alligier et al. 2013, 2014). Furthermore, it serves the purpose of simplifying the computation. Nonetheless, a more informative prior with a skewed distribution can be used, depending on the level of confidence. The fixed variance reduces the computation and simplifies the closed-form solution. However, this is also a minor limitation that future researches would overcome. In other cases of unusual prior distribution, one can still compute the posterior using numerical methods.

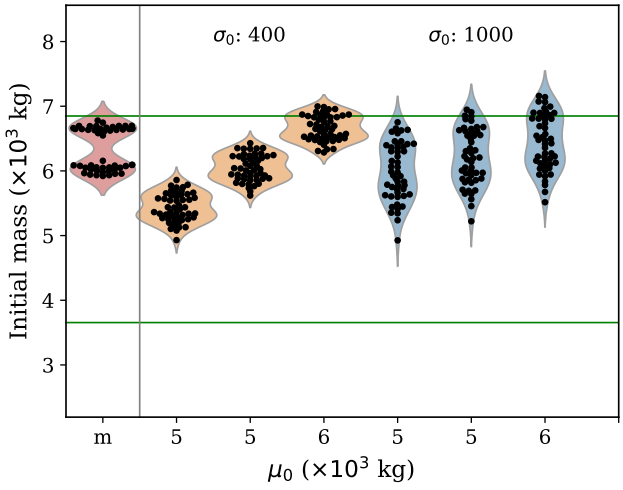

Figure 14: Prior test in relation with the true mass data. Green horizontal lines refer to m_{oew} and m_{mtow}. σ_0 grouped by different colors.

6.2 Mass observations and dealing with partial trajectories

For Bayesian inference, the more *mass observations* are available, the better the quality of the result tends to be. In order to obtain more observations, the long duration of climb and descent can be better utilized. Most of the previous studies tend to consider the climb phase as an entire section for their estimation process. However, the climb and descent phases can be segmented further to create multiple measurements at different flight levels or at several continuous climb/descent segments. The same method in Equation 21 can be applied to obtain more observations to include in the Bayesian inference process.

It is worth noting that each flight in the dataset of this paper contains the complete flight trajectory data that starts before takeoff and lasts until landing is completed. It may include some missed segments during trans-oceanic cruise where no data is available. The completeness of trajectory data is required to be able to use all different mass calculation methods at each flight phase. However, such a condition is not required in order to arrive at a set of estimates. A partial trajectory can be used in the same way, where the number of measurements is simply reduced.

6.3 Uncertainties

As discussed previously for Figure 7, there can be a certain level of variation in the resulting distribution for each individual method. This is expected due to the uncertainty in data, as well as the flight procedures.

Since the mass is tightly linked to the thrust in the total energy model, the uncertainty in thrust will always exists in aircraft mass estimations. This can result a difference between the actual mass and mass computed under maximum thrust profile assumption. On the other hand, using the total energy model, with observed aircraft kinematic states and calculated drag, there are multiple possible thrust and mass combinations. That is, both higher and lower thrust-mass combinations may satisfy the equation at the same time (with different levels of error).

This possibility of the varying thrust is fairly common for aircraft to perform reduced thrust takeoff and climb. Several estimation methods used in this paper require knowledge of the ratio of reduced thrust. That is the rational for using the least squares optimization method in Equation 21. It tries to find the best combination of thrust setting and mass. This approach is similar to previous research by Alligier et al. (2013). In addition, the effect of thrust settings was studied in this paper where difference in mass estimation is found under fixed maximum and minimum thrust profile.

Compared to takeoff and climb, the situation is more complicated in descent. Aircraft trajectories are subjected to more procedures from air traffic controllers. Additionally, different types of continuous descent approaches may be used. Thus, the thrust settings can substantially vary among flights. Optimization according to Equation 21 may not yield the best thrust-mass setting to resemble reality. This effect can be seen in Figure 10 in the descent phase. One possible solution is to reduce the thrust setting range towards idle thrust (per this paper), but doing so may cause those higher-powered descents to suffer a biased result. To over come this drawback, a separate estimation that determine the type of descent can be implemented before the estimation.

Another factor affecting the estimation results is the data quality. With more uncertainties in the aircraft states (position, airspeed, vertical rate), the higher noise returns in the computed *mass observations*. Such fundamental variance can be improved with better quality data (radar data, wind information, or FMS data). However, this variance will always exist in the estimation. To advance the inference using Bayesian methods, investigation in a better error model can be an interesting direction for future studies.

7 Conclusions

In this paper, a new Bayesian inference process for estimating aircraft initial mass was proposed. The core idea of the maximum a posteriori probability (MAP) estimation in Bayesian statistics is to derive estimates by combining mass observations with prior information. The prior is represented as a probability distribution, and the MAP estimate is obtained from the posterior probability distribution. The other major focus of this paper that is presented at the start of the method section is the calculation of multiple initial masses. These are independently computed using data from different flight phases and deterministic methods.

Compared to the deterministic least-squares method presented in previous studies, the extra layer of Bayesian inference that is built on top of different mass observations can ensure improved estimations. This is due to the fact that such a calculation includes the prior knowledge of aircraft mass distribution. This paper tested different hypotheses for the selection of priors, and their influence on the estimation results. It was found that thrust setting and wind can act as important factors that influence the mass estimation.

During initial mass calculations, a simplified fuel burn model was constructed based on the open ICAO emission data bank. For this paper, it provided a means to calculate the total fuel burn at the time when a mass is computed. Under such conditions, it is thus possible to derive the initial mass from this computed mass. This fuel burn model can also be applied in other studies, since the input data is based solely on aircraft surveillance data such as ADS-B or radar data.

To validate the proposed estimation process, data from a set of 50 flights carried out by a Cessna Citation II aircraft was used. True initial masses of these flights were recorded for these flights in the data set. The estimation under a well-defined prior distribution yields a mean absolute error of 4.3% with respect to the true aircraft mass among all flights.

In this paper the Bayesian inference was applied on the level of mass observations. It requires long observation of the flight trajectory and is best suited for post process. It makes the analysis of aircraft performance based on historical data more accurate. However, this extended observation of flight trajectory requirement also poses the major limitation of the method for real-time estimation, where only a small portion of the data may be collected by a single ADS-B receiver. To overcome this limitation, another further step would be integrating the Bayesian estimation to the aircraft performance equations. Under such circumstances, accuracy and prediction time can expected to be improved. At the same time, reduction of wind uncertainty and a better understanding of the thrust settings would also improve this method and bring better estimation results in the future.

References

Alligier, R., Gianazza, D. & Durand, N. (2013), 'Learning the aircraft mass and thrust to improve the ground-based trajectory prediction of climbing flights', *Transportation Research Part C: Emerging Technologies* **36**, 45–60.

Alligier, R., Gianazza, D. & Durand, N. (2015), 'Machine learning and mass estimation methods for ground-based aircraft climb prediction', *IEEE Transactions on Intelligent Transportation Systems* **16**(6), 3138–3149.

Alligier, R., Gianazza, D., Ghasemi Hamed, M. & Durand, N. (2014), Comparison of two ground-based mass estimation methods on real data, *in* '6th International Conference on Research in Air Transportation (ICRAT)'.

Bartel, M. & Young, T. M. (2008), 'Simplified thrust and fuel consumption models for modern two-shaft turbofan engines', *Journal of Aircraft* **45**(4), 1450–1456.

Bayes, T., Price, R. & Canton, J. (1763), *An essay towards solving a problem in the doctrine of chances*, C. Davis, Printer to the Royal Society of London.

Chati, Y. S. & Balakrishnan, H. (2016), Statistical modeling of aircraft engine fuel flow rate, *in* '30th Congress of the International Council of the Aeronautical Science'.

Chatterji, G. B. (2011), Fuel burn estimation using real track data, *in* '11th AIAA ATIO Conference'.

Coppenbarger, R. (1999), En route climb trajectory prediction enhancement using airline flight-planning information, *in* 'Guidance, Navigation, and Control Conference and Exhibit'.

Fleuti, E. & Polymeris, J. (2004), Aircraft nox-emissions within the operational lto cycle, Technical report, Flughafen Zurich AG.

Fricke, H., Seiß, C. & Herrmann, R. (2015), 'Fuel and energy benchmark analysis of continuous descent operations', *Air Traffic Control Quarterly* **23**(1), 83–108.

Gelman, A., Carlin, J. B., Stern, H. S. & Rubin, D. B. (2014), *Bayesian data analysis*, Vol. 2, Chapman & Hall/CRC Boca Raton, FL, USA.

ICAO (2016), 'Aircraft engine emissions databank', *International Civil Aviation Organization* .

Jackson, M. R., Zhao, Y. J. & Slattery, R. A. (1999), 'Sensitivity of trajectory prediction in air traffic management', *Journal of Guidance, Control, and Dynamics* **22**(2), 219–228.

Lee, H.-T. & Chatterji, G. (2010), Closed-form takeoff weight estimation model for air transportation simulation, *in* '10th AIAA Aviation Technology, Integration, and Operations (ATIO) Conference', p. 9156.

Mair, W. A. & Edwards, B. (1965), 'A parametric study of take-off and landing distances for high-lift aircraft', *aeronautical research council* p. C.P. No. 823.

Murphy, K. P. (2007), Conjugate bayesian analysis of the gaussian distribution.

Nuic, A. (2014), 'User manual for the base of aircraft data (bada) revision 3.12', *Atmosphere* **2014**.

Schultz, C., Thipphavong, D. & Erzberger, H. (2012), Adaptive trajectory prediction algorithm for climbing flights, *in* 'AIAA Guidance, Navigation, and Control (GNC) Conference', p. 2.

Sun, J., Ellerbroek, J. & Hoekstra, J. (2016), Modeling and inferring aircraft takeoff mass from runway ads-b data, *in* '7th International Conference on Research in Air Transportation'.

Sun, J., Ellerbroek, J. & Hoekstra, J. (2017*a*), Bayesian inference of aircraft initial mass, *in* 'Proceedings of the 12th USA/Europe Air Traffic Management Research and Development Seminar', FAA/EUROCONTROL.

Sun, J., Ellerbroek, J. & Hoekstra, J. (2017*b*), Modeling aircraft performance parameters with open ads-b data, *in* 'Twelfth USA/Europe Air Traffic Management Research and Development Seminar'.

Thipphavong, D. P., Schultz, C. A., Lee, A. G. & Chan, S. H. (2012), 'Adaptive algorithm to improve trajectory prediction accuracy of climbing aircraft', *Journal of Guidance, Control, and Dynamics* **36**(1), 15–24.

Wetmore, J. (1937), The rolling friction of several airplane wheels and tires and the effect of rolling friction on take-off.